


Research Article

Reconnoitring Wear Resistance and Mechanical Strengths of AA8111/B₄C/ZrO₂ Nanocomposite through Taguchi Route

Sathish Thanakodi,¹ Mohanavel Vinayagam,^{2,3} M. Ravichandran,⁴ T. Raja,⁵ A. H. Seikh,⁶ M. H. Siddique,⁷ and Beruk Hailu ⁸

¹Department of Mechanical Engineering, Saveetha School of Engineering, SIMATS, Chennai, Tamilnadu, India

²Centre for Materials Engineering and Regenerative Medicine, Bharath Institute of Higher Education and Research, Chennai, 600073 Tamil Nadu, India

³Department of Mechanical Engineering, Chandigarh University, Mohali 140413, Punjab, India

⁴Department of Mechanical Engineering, K.Ramakrishnan College of Engineering, Trichy, Tamil Nadu, India

⁵Department of Mechanical Engineering, Vel Tech Rangarajan Dr. Sagunthala R&D Institute of Science and Technology, Chennai, Tamil Nadu, India

⁶Mechanical Engineering Department, College of Engineering, King Saud University, P.O. Box 800, Riyadh 11421, Saudi Arabia

⁷Intelligent Construction Automation Centre, Kyungpook National University, Daegu, Republic of Korea

⁸Faculty of Mechanical Engineering, Haramaya Institute of Technology, Haramaya University, Ethiopia

Correspondence should be addressed to Beruk Hailu; beruk.hailu@haramaya.edu.et

Received 11 May 2022; Accepted 16 July 2022; Published 8 September 2022

Academic Editor: Arpita Roy

Copyright © 2022 Sathish Thanakodi et al. This is an open access article distributed under the Creative Commons Attribution License, which permits unrestricted use, distribution, and reproduction in any medium, provided the original work is properly cited.

Nowadays, the use of aluminium alloys is increasing in all domains of application, including industry, medical, electrical, and household appliances. In general, aluminium alloy is a lightweight material with great strength when compared to other alloys. According to the uses, the aluminium alloy must be strengthened by the inclusion of reinforced particles via the stir casting process. The purpose of this study was to create nanocomposite samples of AA8111/B₄C/ZrO₂ using a stir casting procedure. To prepare nanocomposite samples, the matrix of aluminium alloy AA8111 is supplemented with nanoparticles of boron carbide (B₄C) and zirconium dioxide (ZrO₂) in varied proportions. Optimize the stir casting parameters using a statistical approach such as the Taguchi technique to improve mechanical and wear attributes. The following process parameters were chosen: nanoparticle reinforcement quantity (4% to 10% with the step of 2%), melting temperature (800°C to 950°C with the step of 50°C), stir time (20 min to 35 min with the step of 5 minutes), and stir speed (400 rpm to 550 rpm with the step of 50 rpm). Wear and tensile strength tests are performed; the melting temperature is heavily impacted in the wear test, and the stir speed is heavily influenced in the tensile strength analysis. This experimental effort yielded a minimum wear of 0.085 mm³/m and a maximum ultimate strength of 167.6 N/mm².

1. Introduction

Compared to single material, the combination of different elements presents in the single material possesses extreme strength as well as excellent mechanical properties [1]. Different elements are blended into the base material named as composites materials, more than two materials of mixing called as hybrid composites [2–4]. Composite materials increase its strength while manufacturing the parts. In recent

days, the aluminium alloy material is highly used in the automobile field to satisfy various applications. Making of engine components and the body building of vehicles considered the aluminium alloy vastly due to its light weight and higher strength ratio. Aerodynamic consideration the aluminium alloy is the most wanted material in the aerospace applications; fabrications of wings and body structure are required aluminium alloy [5–7]. Different aluminium alloy series are available, based on the applications the

TABLE 1: AA8111 chemical constituents.

Chemical element	Quantity (%)
Silicon	1.1
Magnesium, mg	0.05
Zinc	0.10
Manganese	0.10
Titanium	0.08
Chromium	0.03
Iron	0.8
Copper	0.10
Aluminium	Remaining.

chosen of aluminium alloy with the main role in the manufacturing process. Household equipment and parts are fabricated by using aluminium alloys at a high rate. Home appliances such as pressure cooker, furniture items, electrical conductors, and packing container in the food processing units highly consumed aluminium alloy [8–10].

Strength of aluminium alloy materials is increased by reinforcing hard particles namely boron carbide, titanium carbide, silicon carbide, zirconium dioxide, aluminium oxide, etc. [11–13]. Reinforced particles boron carbide and zirconium dioxide are blended efficiently to the aluminium alloy which is achieved by powder metallurgy or stir casting process [14]. Using the powder metallurgy technique, the ball milling process was employed in blending the matrix material with reinforcing nanoparticles to obtain the homogeneous mixture. After conducting the ball milling process, the powders are compacted further; the green compact is sintered and extruded for conducting of different mechanical tests [15–17]. Stir casting process is called the liquid metallurgy process; it can be achieved by melting the base material with reinforced particles in the crucible [18, 19]. Stir casting process is improved through the selection of different process parameters. Effective reinforcement is obtained by using the stir casting process; it is a low-cost method for making composite materials [20–22].

In many engineering applications, the quality improvement is attained through statistical approach such as the Taguchi optimization method; it is one of the robust design methods [23, 24]. The Taguchi method is developed by Genichi Taguchi for improving the engineering quality such as the quality of manufacturing goods [25]. Most of the composites are undergone to wear and mechanical properties analysis; these analyses check the reinforcement accumulation and the strength of the composites [26–28]. This experimental work is aimed at fabricating nanocomposite samples of AA8111/B₄C/ZrO₂ through stir casting process and identifying the best performing sample from testing for mechanical strength and wear. Base material and reinforced particles are selected as aluminium alloy (AA8111) and boron carbide/zirconium dioxide, respectively. Taguchi L16 orthogonal array is included to optimize the manufacturing parameter of quantity of reinforcement and process parameters of stir casting process. Responses of this work is considered wear and ultimate tensile stress.

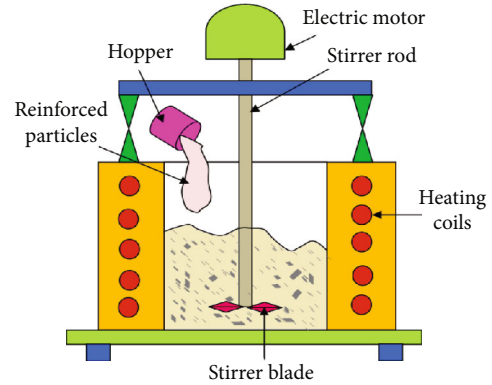


FIGURE 1: Stir casting setup.



FIGURE 2: Wear test specimen.

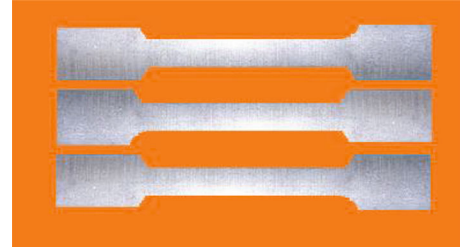


FIGURE 3: Tensile test specimens.

TABLE 2: AA8111/B₄C/ZrO₂ nanocomposite synthesizing variables and levels.

S. No.	Composites and testing parameters	Input levels			
		1	2	3	4
1.	Stir time (min) (ST)	20	25	30	35
2.	Melting temperature (°C) (MT)	800	850	900	950
3.	Stir speed (rpm) (SS)	400	450	500	550
4.	Nanoparticle reinforcement (%) (NPR)	3	6	9	12

2. Materials and Methods

Aluminium alloy AA8111 is the wrought alloy category; it possesses high strength, and hence, the base material was AA8111. The nanoreinforcement particles are zirconium

TABLE 3: Experimental observations' summary of ultimate tensile stress test and wear test.

Exp. runs	Reinforcement (%)	Stir speed (rpm)	Stir time (min)	Melting temperature (°C)	Wear rate (mm ³ /m)	Predicted Wear rate (mm ³ /m)	Ultimate tensile stress (N/mm ²)	Predicted ultimate tensile stress (N/mm ²)
1	4	400	20	800	0.234	0.258	95.2	98.065
2	4	450	25	850	0.303	0.310	112.3	110.815
3	4	500	30	900	0.219	0.362	132.7	123.565
4	4	550	35	950	0.520	0.414	124.2	136.315
5	6	400	25	900	0.085	0.231	78.3	102.870
6	6	450	20	950	0.314	0.164	121.1	96.340
7	6	500	35	800	0.610	0.647	155.8	159.170
8	6	550	30	850	0.544	0.580	163.0	152.640
9	8	400	30	950	0.316	0.282	120.3	115.375
10	8	450	35	900	0.533	0.490	145.7	143.525
11	8	500	20	850	0.655	0.460	124.3	133.115
12	8	550	25	800	0.747	0.668	161.7	161.265
13	10	400	35	850	0.573	0.568	153.2	150.980
14	10	450	30	800	0.686	0.656	167.6	159.850
15	10	500	25	950	0.395	0.433	129.5	137.920
16	10	550	20	900	0.318	0.522	143.7	146.790

TABLE 4: Signal-to-noise ratios for the observations of wear test.

Level	Nanoparticle reinforcement (%)	Stir speed on the melt (rpm)	Time duration of stirring (min)	Melting temperature (°C)
1	10.459	12.231	9.081	5.674
2	10.271	7.289	10.596	6.037
3	5.418	7.301	7.940	12.514
4	6.533	5.861	5.065	8.456
Delta	5.040	6.369	5.531	6.840
Rank	4	2	3	1

dioxide and boron carbide based on their appreciable qualities in improving mechanical and wear strengths [29]. Base material is procured from Sargam Metals Private Limited, Chennai, and reinforced particles are purchased from Ashoka Marketing Agencies, Chennai, with required quantity for conducting of experiments. Table 1 presents the chemical constituents of the AA8111 aluminium alloy and its density is 2.71 g/cc.

The method for synthesizing the samples of the proposed nanocomposite is the stir casting process. The aim this research is to improve the mechanical strengths and wear resistance by hybrid reinforcement of nanoparticles of B₄C and ZrO₂. The objectives of the research are synthesizing nanocomposite samples by varying reinforcement percentage and manufacturing parameters like stirring speed, stir time, and melting time. Statistical approach such as Taguchi methodology is concentrated for this experimental to optimize reinforcement quantity as well as parameters of the stir casting to fabricate best nanocomposite. The main motivation to implement L₁₆ is based on the four-level factors in the selected parameters.

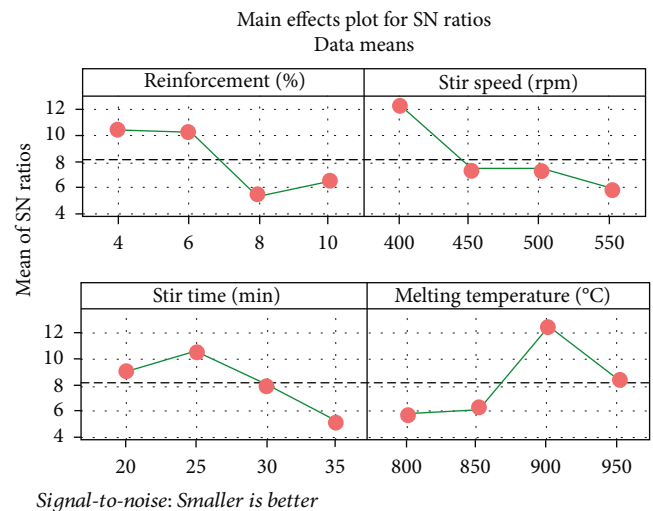


FIGURE 4: Main effects plot for S/N ratio (wear test).

TABLE 5: Analysis of variance (wear test).

Source	DF	Seq SS	Contribution	Adj SS	Adj MS	F value	P value
Regression	4	0.38866	69.51%	0.38866	0.09717	6.27	0.007
Reinforcement of nanoparticles	1	0.09687	17.32%	0.09687	0.09687	6.25	0.030
Stirring speed	1	0.09894	17.69%	0.09894	0.09894	6.38	0.028
Stirring duration	1	0.07103	12.70%	0.07103	0.07103	4.58	0.056
Melting temperature	1	0.12182	21.79%	0.12182	0.12182	7.86	0.017
Error	11	0.17049	30.49%	0.17049	0.01550		
Total	15	0.55915	100.00%				

TABLE 6: Optimization process input (wear test).

Response	Weight	Lower	Upper	Target	Goal	Importance
Rate of wear (mm^3/m)	1		0.7475	0.0847	Minimum	1

TABLE 7: Optimization process results (wear test).

Solution	Reinforcement (%)	Stirring speed	Stirring time	Melting temperature ($^{\circ}\text{C}$)	Wear rate (mm^3/m) fit	Composite desirability
1	4	400	20	950	0.0245325	1

3. Experimental Procedure

The reinforcement nanoparticles are blended at a predefined quantity with the AA8111 powder in a ball mill. Then homogeneous mixture was preheated through furnace separately; heating and melting are achieved by stir casting process. Different elements are melted simply by using the stir casting, and the bottom pouring furnace is considered for this work [30, 31]. The schematic diagram of the stir casting process with key components is furnished as shown in Figure 1.

Initially, the different weight percentages (4% to 10% with the step of increment 2%) of the ZrO_2 and B_4C with equal share were preheated in the furnace. The main advantages of the preheating process are improving the mixture rate and removing the unwanted impurities present in the elements of the reinforced particles. The preheating process is carried out 550°C for 4 hours in the crucible. The base material of the AA8111 is heated at an elevated temperature of 950°C continuously with the aid of bottom pouring furnace. The preheated reinforced molten material is poured into the molten base material; further, the different temperature levels (800°C , 550°C , 900°C , and 950°C) are maintained for melting the blended mixture. Also, the different stir time (20 min to 35 min with the step of increment 5 min) and stir speed (400 rpm, 450 rpm, 500 rpm, and 550 rpm) are considered for achieving homogeneous mixture. Finally, the melted materials are poured into the selected die and received the samples for conducting wear and mechanical tests.

3.1. Wear Test. The standard of ASTM G99 was followed to conduct the wear test. The samples were prepared the dimensions of 12 mm diameter and 35 mm length as shown in Figure 2.

The DUCOM dry sliding wear test apparatus is employed in investigating the wear property. The weight loss is measured by weighing the sample before and after the test. Wear test parameters are as follows: sliding distance of 1500 m, applied load of 40 N, and sliding velocity of 3 m/s were set for testing all specimens.

3.2. Tensile Test. The tensile test is conducted through universal testing machine (UTM) as per the ASTM E8 standard $100 \times 20 \times 5$ mm, and the tensile test specimens' image is illustrated in Figure 3. Specimen is fixed in between the jaws, and load is applied uniformly; at the same time, the strain was measured using an extensometer. Finally, the specimen is broken, and its dimensions are measured. The stir casting parameters and their levels are tabulated in Table 2.

4. Results and Discussion

Table 3 shows the experimental output for the tensile stress test and wear test. The minimum wear was observed at $0.085 \text{ mm}^3/\text{m}$ obtained at the parameter's levels of 900°C of melting temperature, 25 min of stir time, 400 rpm of stir speed, and 4% of nanoparticle reinforcement. In ultimate tensile stress analysis, the maximum ultimate tensile stress occurred at 167.6 N/mm^2 by involving 10% of reinforcement, 450 rpm of stir speed, 800°C molten temperature, 30 min of stir time, and 450 rpm of stir speed.

It was observed in Table 4 that the signal-to-noise ratio for wear test observations, the highly influencing factor, is melting temperature, the next was stir speed, and stir time and percentage of nanoparticle reinforcement are in the ranking order. The high signal was obtained for nanoparticle reinforcement contribution of 4%. In the case of stirring speed level 1400 rpm, the factor of stir time is 25 minutes, and the favourable melting temperature was 900 as shown in Figure 4.

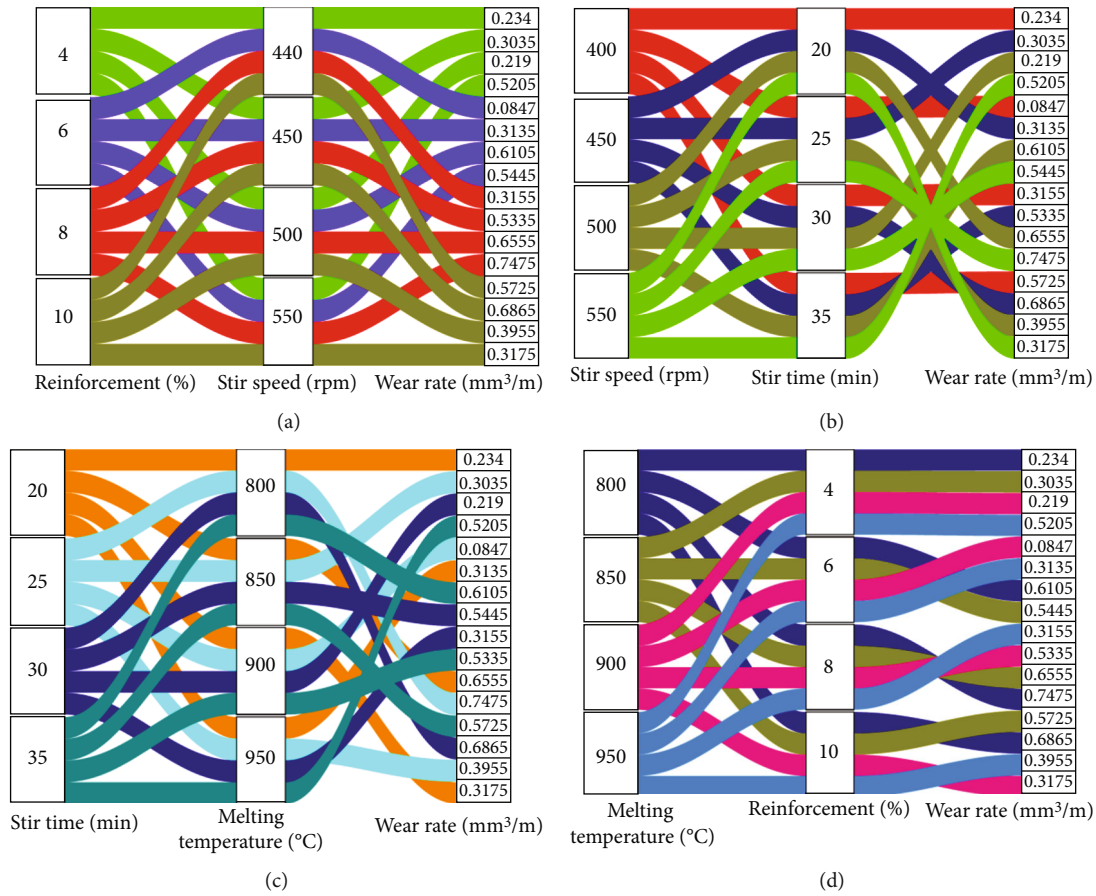


FIGURE 5: Parallel set plots: (a) stirring speed vs. reinforcement nanoparticles (%); (b) stirring time vs. stirring speed; (c) melting temperature vs. stir time; and (d) reinforcement nanoparticles (%) vs. melting temperature.

The minimum reinforcement percentage offered a minimum wear rate, improving the reinforcement percentage that increases the rate of wear of nanocomposite. Similarly, increasing the stir speed increases the wear rate. The minimum wear rate could be achieved at 400 rpm of stir speed offered at minimum. In consideration of the stir time, the 25 min duration resulted in the less rate of wear. Further, increasing the stir time, the wear rate also increases. Increasing the melting temperature decreases the wear rate, and 900°C of melting temperature offered a minimum wear rate.

Table 5 presents the contribution of each parameters in the wear test, and the melting temperature highly contributed as 21.79% compared to the remaining parameters. Stir speed contributed as 17.69%, reinforcement percentage contributed as 17.32%, and stir time contributed as 12.70%. Fisher’s value was estimated with the higher contribution levels.

4.1. Regression Equation.

$$\text{Wear rate (mm}^3/\text{m)} = 0.567 - 0.001561\text{MT} + 0.001407\text{SS} + 0.0348\text{NPR} + 0.01192\text{ST}. \tag{1}$$

Tables 6 and 7 illustrate the input and results of the optimization process; the optimized rate of wear is 0.0245 mm³/

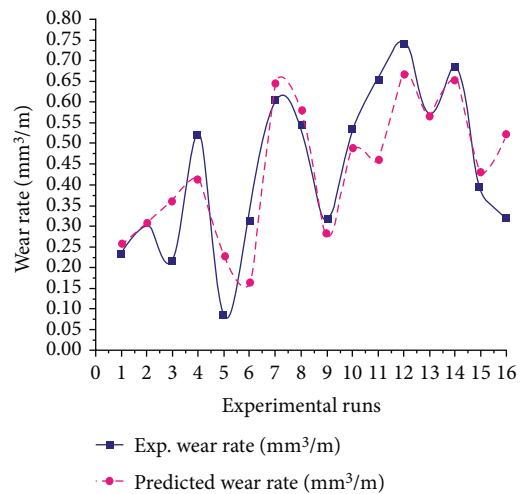


FIGURE 6: Experimental runs vs. wear rate (experimental and predicted).

m at the condition of 950°C of melting temperature by 400 rpm of stir speed, 4% of reinforcement, and 20 min of stir time as shown in Equation (1).

Figure 5 exhibits the correlation between two parameters based on the analysis. The relationship between nanoparticle

TABLE 8: Signal-to-noise ratios results of Taguchi for the observations of ultimate tensile stress.

Level	Reinforcement (%)	Stir speed (rpm)	Stir time (min)	Melting temperature (°C)
1	41.23	40.69	41.57	43.02
2	41.91	42.61	41.33	42.71
3	42.73	42.61	43.20	41.69
4	43.40	43.36	43.18	41.85
Delta	2.17	2.67	1.87	1.33
Rank	2	1	3	4

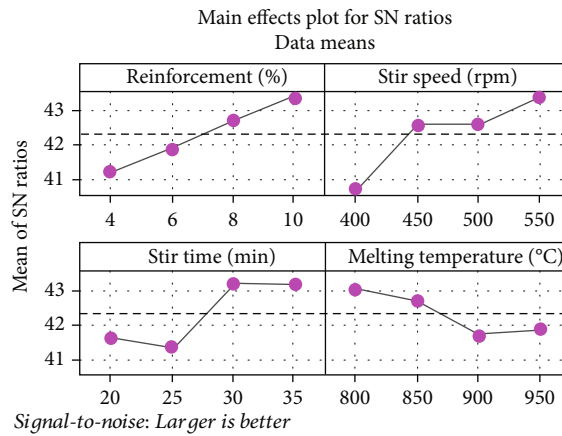


FIGURE 7: Main effects plot for S/N ratio (ultimate tensile stress test).

TABLE 9: Analysis of variance for ultimate tensile stress analysis.

Source	DF	Seq SS	Contribution	Adjusted sum of squares	Adjusted mean square	F value	P value
Regression	4	7614	80.64%	7614	1903.5	11.45	0.001
Reinforcement (%)	1	2232	23.64%	2232	2232.4	13.43	0.004
Stir speed (rpm)	1	2337	24.75%	2337	2337.1	14.06	0.003
Stir time (min)	1	1859	19.68%	1859	1858.6	11.18	0.007
Melting temperature (°C)	1	1186	12.56%	1186	1185.8	7.13	0.022
Error	11	1828	19.36%	1828	166.2		
Total	15	9442	100.00%				

reinforcement (%) and stir speed is shown in Figure 5(a). The minimum wear is observed at the condition of 400 rpm of stir speed and 6% of nanoparticle reinforcement. Figure 5(b) represents that associations among stir time and stir speed, from that 25 min of stirring time duration and 400 rpm of stir speed, offered a minimum wear rate. Figure 5(c) illustrates the connection between stir time and melting temperature, in that the 900°C of melting temperature and 25 min of stirring time duration recorded less rate of wear. Figure 5(d) correlates the melting temperature and reinforcement percentage, 6% of nanoparticle reinforcement, and 900°C of melting temperature registered as the minimum wear rate.

The association among predicted and experimental wear rate is depicted in Figure 6. Many of the observations from

experiment were occupied in between the range of predicted values spread; hence, the preferred model and data points were sufficient for conducting wear test.

From the ultimate tensile stress analysis, the stir speed was extremely involved due to the rank order as presented in Table 8. Further, the reinforcement percentage, stir time, and melting temperature are ranked accordingly based on the influence on the UTS. The higher UTS recorded at the levels of factors are as follows: 550 rpm of stir speed, 800°C of melting temperature, 30 min of stirring time, and 10% of nanoparticle reinforcement.

The highest reinforcement percentage (10%) and stir speed (550 rpm) recorded the maximum ultimate tensile stress as shown in Figure 7. Increasing the stir time from 20 min to 30 min, the ultimate tensile stress was increased.

TABLE 10: Optimization process input (ultimate tensile stress).

Response	Goal	Lower	Target	Upper	Weight	Importance
Ultimate tensile stress (N/mm ²)	Maximum	78.3	167.6		1	1

TABLE 11: Optimization process results (ultimate tensile stress).

Solution	Reinforcement (%)	Stir speed (rpm)	Stir time (min)	Melting temperature (°C)	Ultimate tensile stress (N/mm ²) fit	Composite desirability
1	10	550	35	800	191.11	1

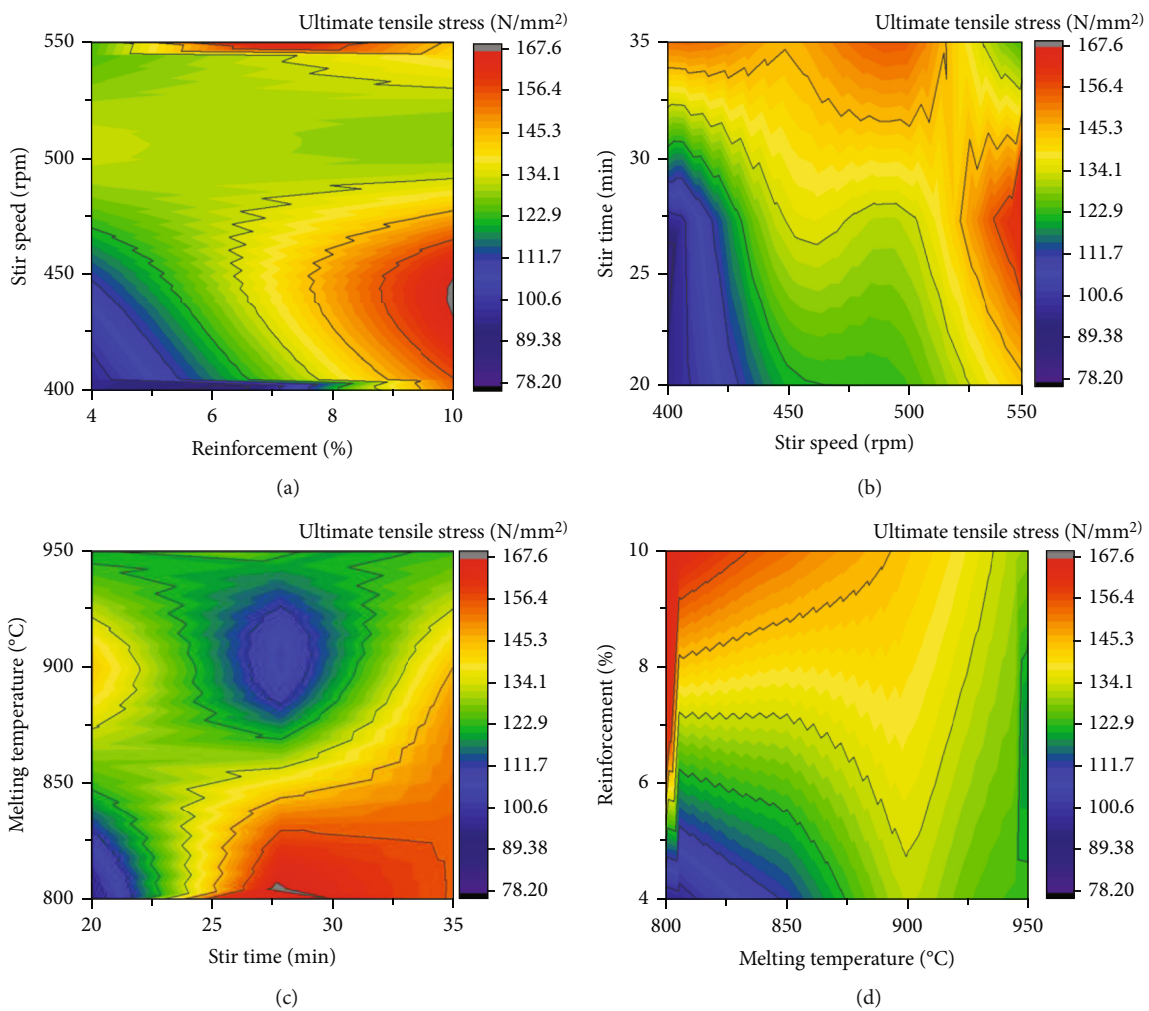


FIGURE 8: Contour plots: (a) stirring speed vs. percentage of nanoparticle reinforcement; (b) stirring duration (time) vs. stirring speed; (c) melting temperature vs. stirring duration (time); (d) percentage of nanoparticle reinforcement vs. melting temperature.

The minimum melting temperature of 800°C recorded the maximum ultimate tensile stress.

Stir speed (24.75%) was highly contributed in the ultimate tensile stress, followed by reinforcement (%) (23.64%), stir time (19.68%), and melting temperature (12.56%). All the contribution was decided by the F value, and a higher F value denoted the higher contribution in the ultimate tensile stress. The contribution of factors on UTS could be obtained from Table 9 based on the F value.

4.2. Regression Equation.

$$\begin{aligned} \text{Ultimate tensile strength (N/mm}^2\text{)} \\ = 75.1 + 1.928\text{ST} - 0.1540\text{MT} + 5.28\text{NPR} + 0.2162\text{SS} \end{aligned} \quad (2)$$

Tables 10 and 11 illustrate the input and results of the optimization process, the optimized ultimate tensile stress

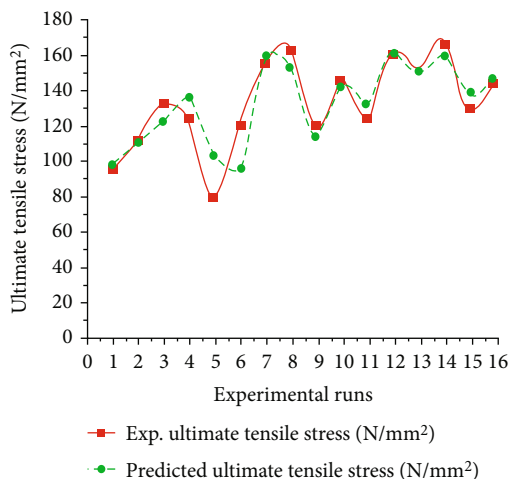


FIGURE 9: Experimental runs vs. ultimate tensile stress.

was registered as $191.110.0245 \text{ N/mm}^2$ by 800°C of melting temperature, 35 min of stir time, 550 rpm of stir speed, and 10% of nanoparticle reinforcement as shown in Equation (2).

The correlation between two parameters for the response of ultimate tensile stress is shown in Figure 8. Figure 8(a) shows the associations between reinforcement (%) and stir speed. The maximum ultimate tensile stress was noticed at the point with the nanoparticle reinforcement of 10% and stirring speed of 450 rpm. Figure 8(b) signifies the correlation between the speed of stirring while synthesizing the nanocomposite and the stirring time duration. Hence, the optimal condition is 30 min of stirring time, and the stirring speed of 550 rpm was recorded the maximum ultimate tensile stress. Figure 8(c) explains the correlation among stirring durations (time) and melting temperature, in that 800°C of melting temperature and stirring time was 30 min of the registered maximum ultimate tensile stress. Figure 8(d) illustrates the melting temperature and reinforcement percentage; hence, 10% of nanoparticle reinforcement with 800°C of melting temperature is the maximum ultimate tensile stress.

Figure 9 shows the relationship between experimental and predicted ultimate tensile stress. From this analysis, many experimental observations were fall within the range of predicted values; hence, the chosen model and data points were adequate for conducting ultimate tensile stress.

5. Conclusion

Using the stir casting process, the aluminium metal matrix (AMMCs) composites ($\text{AA8111} + \text{B}_4\text{C}/\text{ZrO}_2$) were produced successfully, and the stir casting process parameters were optimized. Finally, the minimum wear and maximum ultimate tensile stress was obtained through statistical analysis; the results were concluded as the follows:

- (i) Based on the wear test analysis, the minimum wear was found to be $0.085 \text{ mm}^3/\text{m}$ when 4 percent of nanoparticle reinforcement, 400 rpm stir speed, 25 min stir time, and 900°C melting temperature were all used. In the ultimate tensile stress study,

the maximum ultimate tensile stress was recorded as 167.6 N/mm^2 when 10% reinforcement, 450 rpm stir speed, 30 min stir duration, and 800°C molten temperature were used

- (ii) In the wear test, the best results were obtained with a 4 percent reinforcement, 400 rpm stir speed, 25 minute stir time, and a molten temperature of 900°C . In the same way, the best parameters for ultimate tensile stress analysis were 10% reinforcement, 550 rpm stir speed, 30 min stir time, and 800°C melting temperature
- (iii) From the wear test, the higher contribution was achieved as 21.79% by melting temperature contrast to remaining parameters. Stir speed contributed as 17.69%, reinforcement percentage contributed as 17.32%, and stir time contributed as 12.70%. In the ultimate tensile stress analysis, maximum contribution (24.75%) was reached by stir speed followed by reinforcement (%) (23.64%), stir time (19.68%), and melting temperature (12.56%)
- (iv) In the optimization process analysis, the minimum wear rate was registered as $0.0245 \text{ mm}^3/\text{m}$ at 950°C of melting temperature 400 rpm of stir speed, 4% of reinforcement percentage, and 20 min of stir time. Similarly, the optimized ultimate tensile stress was recorded as 191.11 N/mm^2 by 800°C of melting temperature, 550 rpm of stir speed, 10% of reinforcement percentage, and 35 min of stir time

Data Availability

The data used to support the findings of this study are included within the article. Further data or information is available from the corresponding author upon request.

Conflicts of Interest

The authors declare that there are no conflicts of interest regarding the publication of this paper.

Acknowledgments

The authors appreciate the supports from Haramaya University, Ethiopia, for the research and preparation of the manuscript. The authors thank Saveetha School of Engineering, SIMATS, K.Ramakrishnan College of Engineering, and Chandigarh University, for providing assistance to this work. The authors would like to acknowledge the Researchers Supporting Project Number (RSP-2021/373), King Saud University, Riyadh, Saudi Arabia.

References

- [1] Y. Pazhouhanfar and B. Eghbali, "Microstructural characterization and mechanical properties of TiB_2 reinforced Al6061 matrix composites produced using stir casting process," *Materials Science and Engineering: A*, vol. 710, pp. 172–180, 2018.

- [2] V. Mohanavel and M. Ravichandran, "Optimization of parameters to improve the properties of AA7178/Si3N4 composites employing Taguchi approach," *Silicon*, vol. 14, no. 4, pp. 1381–1394, 2022.
- [3] C. Jia, P. Zhang, X. Wenrui, and W. Wang, "Neutron shielding and mechanical properties of short carbon fiber reinforced aluminium 6061-boron carbide hybrid composite," *Ceramics International*, vol. 47, no. 7, pp. 10193–10196, 2021.
- [4] J. A. Jeffrey, S. S. Kumar, P. Hariharan, M. Kamesh, and A. M. Raj, "Production and assessment of AZ91 reinforced with nano SiC through stir casting process," *Materials Science Forum*, vol. 1048, pp. 9–14, 2022.
- [5] M. Dhanashekar, P. Loganathan, S. Ayyanar, S. R. Mohan, and T. Sathish, "Mechanical and wear behaviour of aa6061/sic composites fabricated by powder metallurgy method," *Materials Today: Proceedings*, vol. 21, pp. 1008–1012, 2020.
- [6] S. Murali, A. Chockalingam, S. Suresh Kumar, and M. Remanan, "Production, characterization and friction stir processing of AA6063-T6/Al3Tip in-situ composites," *International Journal of Mechanical and Production Engineering Research and Development*, vol. 2018, pp. 399–406, 2018.
- [7] N. R. J. Hynes, S. Raja, R. Tharmaraj, C. I. Pruncu, and D. Dispinar, "Mechanical and tribological characteristics of boron carbide reinforcement of AA6061 matrix composite," *Journal of the Brazilian Society of Mechanical Sciences and Engineering*, vol. 42, no. 4, pp. 1–11, 2020.
- [8] J. Zhu, W. Jiang, G. Li, F. Guan, Y. Yang, and Z. Fan, "Microstructure and mechanical properties of SiC_{np}/Al6082 aluminum matrix composites prepared by squeeze casting combined with stir casting," *Journal of Materials Processing Technology*, vol. 283, article 116699, 2020.
- [9] K. Halil, O. İsmail, D. Sibel, and Ç. Ramazan, "Wear and mechanical properties of Al6061/SiC/B₄C hybrid composites produced with powder metallurgy," *Journal of Materials Research and Technology*, vol. 8, no. 6, pp. 5348–5361, 2019.
- [10] A. H. Idrisi and A.-H. I. Mourad, "Conventional stir casting versus ultrasonic assisted stir casting process: mechanical and physical characteristics of AMCs," *Journal of Alloys and Compounds*, vol. 805, pp. 502–508, 2019.
- [11] T. Sathish, V. Mohanavel, K. Ansari et al., "Synthesis and characterization of mechanical properties and wire cut EDM process parameters analysis in AZ61 magnesium alloy+ B4C+ SiC," *Materials*, vol. 14, no. 13, p. 3689, 2021.
- [12] P. Madhukar, N. Selvaraj, R. Gujjala, and C. S. P. Rao, "Production of high performance AA7150-1% SiC nanocomposite by novel fabrication process of ultrasonication assisted stir casting," *Ultrasonics Sonochemistry*, vol. 58, article 104665, 2019.
- [13] N. Faisal and K. Kumar, "Mechanical and tribological behaviour of nano scaled silicon carbide reinforced aluminium composites," *Journal of Experimental Nanoscience*, vol. 13, Supplement 1, pp. S1–S13, 2018.
- [14] H. A. Al-Salihi, A. A. Mahmood, and H. J. Alalkawi, "Mechanical and wear behavior of AA7075 aluminum matrix composites reinforced by Al₂O₃ nanoparticles," *Nano*, vol. 5, no. 3, pp. 67–73, 2019.
- [15] C. A. Chairman, M. Ravichandran, V. Mohanavel et al., "Mechanical and abrasive wear performance of titanium dioxide filled woven glass fibre reinforced polymer composites by using Taguchi and EDAS approach," *Materials*, vol. 14, no. 18, p. 5257, 2021.
- [16] M. A. Taha, R. A. Youness, and M. F. Zawrah, "Review on nanocomposites fabricated by mechanical alloying," *International Journal of Minerals, Metallurgy, and Materials*, vol. 26, no. 9, pp. 1047–1058, 2019.
- [17] M. A. Taha, R. A. Youness, and M. A. Ibrahim, "Evolution of the physical, mechanical and electrical properties of sic-reinforced Al 6061 composites prepared by stir cast method," *Biointerface Research in Applied Chemistry*, vol. 11, pp. 8946–8956, 2020.
- [18] K. Gajalakshmi, N. Senthilkumar, B. Mohan, and G. Anbuezhayan, "An investigation on microstructure and mechanical behaviour of copper-nickel coated carbon fibre reinforced aluminium composites," *Materials Research Express*, vol. 7, no. 11, article 115701, 2020.
- [19] G. Anbuezhayan, B. Mohan, N. Senthilkumar, and R. Pugazhenthii, "Synthesis and characterization of silicon nitride reinforced Al-Mg-Zn alloy composites," *Metals and Materials International*, vol. 27, no. 8, pp. 3058–3069, 2021.
- [20] A. Munimathan, T. Sathish, V. Mohanavel et al., "Investigation on heat transfer enhancement in microchannel using Al₂O₃/water nanofluids," *International Journal of Photoenergy*, vol. 2021, Article ID 6680627, 9 pages, 2021.
- [21] M. Malaki, W. Xu, A. K. Kasar et al., "Advanced metal matrix nanocomposites," *Metals*, vol. 9, no. 3, p. 330, 2019.
- [22] K. Bhoi, H. S. Neeraj, and S. Pratap, "Synthesis and characterization of zinc oxide reinforced aluminum metal matrix composite produced by microwave sintering," *Journal of Composite Materials*, vol. 54, no. 24, pp. 3625–3636, 2020.
- [23] T. Sathish and N. Sabarirajan, "Synthesis and optimization of AA 7175-zirconium carbide composites machining parameters," *Journal of New Materials for Electrochemical Systems*, vol. 24, no. 1, pp. 34–37, 2021.
- [24] P. Mohanty, R. Mahapatra, C. H. Payodhar Padhi, V. V. Ramana, and D. K. Mishra, "Ultrasonic cavitation: an approach to synthesize uniformly dispersed metal matrix nanocomposites—a review," *Nano-Structures & Nano-Objects*, vol. 23, article 100475, 2020.
- [25] S. Thirumalvalavan and N. Senthilkumar, "Experimental investigation and optimization of hvof spray parameters on wear resistance behaviour of Ti-6Al-4V alloy," *Comptes Rendus de l'Academie Bulgare Des Sciences*, vol. 72, no. 5, pp. 665–674, 2019.
- [26] P. R. Jadhav, B. R. Sridhar, M. Nagaral, and J. I. Harti, "Mechanical behavior and fractography of graphite and boron carbide particulates reinforced A356 alloy hybrid metal matrix composites," *Advanced Composites and Hybrid Materials*, vol. 3, no. 1, pp. 114–119, 2020.
- [27] S. Hossain, M. D. Mamunur Rahman, D. Chawla et al., "Fabrication, microstructural and mechanical behavior of Al- Al₂O₃-SiC hybrid metal matrix composites," *Materials Today: Proceedings*, vol. 21, pp. 1458–1461, 2020.
- [28] P. Gurusamy, T. Sathish, V. Mohanavel et al., "Finite Element Analysis of Temperature Distribution and Stress Behavior of Squeeze Pressure Composites," *Advances in Materials Science and Engineering*, vol. 2021, Article ID 8665674, 9 pages, 2021.
- [29] M. Y. Zhou, L. B. Ren, L. L. Fan et al., "Progress in research on hybrid metal matrix composites," *Journal of Alloys and Compounds*, vol. 838, article 155274, 2020.
- [30] M. M. Ravikumar, S. Suresh Kumar, R. Vishnu Kumar, S. Nandakumar, J. Habeeb Rahman, and J. Ashok Raj,

“Evaluation on mechanical behavior of AA2219/SiO₂ composites made by stir casting process,” *AIP Conference Proceedings*, vol. 2405, article 050010, 2022.

- [31] N. K. Bhoi, H. Singh, and S. Pratap, “Developments in the aluminum metal matrix composites reinforced by micro/nano particles—a review,” *Journal of Composite Materials*, vol. 54, no. 6, pp. 813–833, 2020.